EUROPEAN ORGANIZATION FOR NUCLEAR RESEARCH

CERN-PPE/94–89
10 June 1994

Measurement of the B^0-$\bar{B}^0$ Mixing Parameter and the $Z \rightarrow b\bar{b}$ Forward-Backward Asymmetry

The L3 Collaboration

Abstract

We have measured the time integrated B^0-$\bar{B}^0$ mixing parameter and the forward-backward asymmetry in the process $e^+e^- \rightarrow b\bar{b}$ using hadronic events containing muons or electrons. The data sample corresponds to 1,044,000 hadronic decays of the Z. From a fit to the momentum and transverse momentum distributions for single lepton and dilepton events, we have determined the B^0-$\bar{B}^0$ mixing parameter to be

$$\chi_{_B} = 0.123 \pm 0.012\ (\mathrm{stat.}) \pm 0.008\ (\mathrm{sys.}),$$

and the $b\bar{b}$ forward-backward asymmetry at the effective center-of-mass energy $\sqrt{s} = 91.30$ GeV to be

$$A_{b\bar{b}} \quad = \quad 0.087 \pm 0.011\ (\mathrm{stat.}) \pm 0.004\ (\mathrm{sys.}).$$

This measurement corresponds to a value of the effective electroweak mixing angle of

$$\sin^2\overline{\theta}_W = 0.2335 \pm 0.0021.$$

(Submitted to Physics Letters B)

Introduction

The forward-backward asymmetry of quark pairs, $A_{q\bar{q}}$, produced in the process $e^+e^- \rightarrow Z \rightarrow q\bar{q}$ is sensitive to the electroweak mixing angle, $\sin^2\overline{\theta}_W$, which is one of the fundamental parameters of the Standard Model [1]. Within the framework of the improved Born approximation [2,3], the asymmetry on the Z peak is given by

$$A^0_{q\bar{q}} = \frac{3}{4}\frac{2v_e a_e}{v_e^2+a_e^2}\frac{2v_q a_q}{v_q^2+a_q^2}, \tag{1}$$

where v_i is the vector and a_i the axial-vector coupling constant of the electron or quark. The angular distribution of the quark production is

$$\frac{d\sigma}{d\cos\theta} \propto \frac{3}{8}(1+\cos^2\theta) + A_{q\bar{q}}\cos\theta, \tag{2}$$

where θ is the polar angle of the quark with respect to the electron beam direction.

The mixing parameter, χ_B, measures the rate at which a B^0_d or B^0_s meson oscillates into its antiparticle. In the Standard Model this transformation proceeds via a weak flavour-changing box diagram, dominated by virtual top quark exchange. The rate of mixing depends on the Cabibbo-Kobayashi-Maskawa (CKM) matrix elements, V_{td} and V_{ts}, and the top quark mass. The mixing parameter χ_B varies in the range 0.0 to 0.5.

Due to mixing in the B^0-$\bar{B}^0$ system, the b quark asymmetry, $A_{b\bar{b}}$, is related to the observed asymmetry, $A^{obs}_{b\bar{b}}$, by

$$A_{b\bar{b}} = A^{obs}_{b\bar{b}}/(1-2\chi_B). \tag{3}$$

In this letter we present updated measurements of χ_B and $A_{b\bar{b}}$. We use electrons and muons from the semileptonic decay of b quarks to select events coming from $Z \rightarrow b\bar{b}$. Because of the hard fragmentation and large mass of the b quark, leptons from b-quark decay have large momentum, p, and large transverse momentum, p_t, with respect to the quark direction. As the charge of the lepton is correlated with the charge of the quark, we can use events containing these leptons to measure $A_{b\bar{b}}$ and χ_B. We use the thrust axis of the event to estimate the direction of the quark, and we tag its charge with the lepton charge. Similar analyses have previously been reported [4–8]. Our data sample consists of 1,044,000 hadronic events corresponding to an integrated luminosity of 38.9 pb^{-1} collected between 1990 and 1992 on or near the Z resonance using the L3 detector at LEP. The center-of-mass energies were distributed over the range $88.2 \leq \sqrt{s} \leq 94.2$ GeV. Most of the data (91%) was taken at the Z peak, *i.e.* 91.30 GeV.

The L3 Detector

The L3 detector consists of a central tracking chamber, a high resolution electromagnetic calorimeter composed of BGO crystals, a ring of scintillation counters, a uranium and brass hadron calorimeter with proportional wire chamber readout, and an accurate muon chamber system. These detectors are installed in a 12 m diameter magnet which provides a uniform field of 0.5 T along the beam direction.

The central tracking chamber is a time expansion chamber which consists of two cylindrical layers of 12 and 24 sectors, with a total of 62 wires measuring the R-ϕ coordinate. The single wire resolution ranges from 35 μm to 100 μm depending on the drift distance. The transverse momentum resolution is on average $\frac{\sigma(p_t)}{p_t} = 0.018 p_t$ where p_t is in GeV. The fine segmentation of the electromagnetic and hadronic calorimeters allows us to measure the direction of jets with an angular resolution of 2.1° [9], and to measure the total energy of hadronic events from Z decay with a resolution of 10%. The muon detector consists of 3 layers of precise drift chambers which measure 56 points on the muon trajectory in the bending plane and 8 points in the non-bending direction. A detailed description of each detector subsystem and its performance is given in Reference 10.

Event Selection

The trigger requirements and the selection criteria for hadronic events containing electrons or muons have been described previously [11,12]. Muons are identified and measured in the muon chamber system. We require that a muon track consists of track segments in at least two of the three layers of muon chambers, and that the muon track points back to the intersection region. Electrons are identified using the electromagnetic and hadron calorimeters, as well as the central tracking chamber. We require an energy cluster that is consistent with the shape of an electromagnetic shower and which matches in azimuthal angle and momentum with a track in the central tracking chamber. For this analysis, we have only considered electrons in the barrel region ($|\cos\theta| < 0.69$). We reject hadrons misidentified as electrons by requiring that there be less than 3 GeV deposited in the hadron calorimeter in a cone of half angle 7° behind the electromagnetic cluster. The charge of the electron is determined from the track curvature. The shower shape and hadron calorimeter criteria select electrons that are isolated from nearby particles, resulting in a lower efficiency for electrons than for muons.

The momentum of muon candidates is required to be at least 4 GeV, while the electrons are required to have at least 3 GeV. In addition, to increase the $b\bar{b}$ purity, the transverse momentum of the lepton is required to be at least 1 GeV. The transverse momentum is defined with respect to the nearest jet [9], where the measured energy of the lepton is excluded from the jet. The event is rejected if there is no jet with an energy greater than 6 GeV remaining in the same hemisphere as the lepton.

Table 1 shows the number of single lepton and dilepton events obtained after all cuts. The single lepton sample is used to determine the asymmetry, while the dilepton sample with the leptons in opposite hemispheres is used to measure the mixing parameter.

Type	Total Events	Events with ≥ 2 Leptons			
		Opposite Hemisphere		Same Hemisphere	
		Same sign	Opposite Sign	Same sign	Opposite Sign
μ + hadrons	24027				
e + hadrons	10696				
$\mu\mu$ + hadrons	857	210	427	22	198
ee + hadrons	216	46	114	2	54
μe + hadrons	766	193	402	25	146

Table 1: Number of inclusive lepton and dilepton events.

Monte Carlo Models

We use the JETSET 7.3 Monte Carlo program [13] to simulate both the fragmentation and the decay for hadronic events. The events are passed through the full L3 detector simulation [14], which includes the effects of experimental resolution, energy loss, multiple scattering, interactions and decays in the detector materials as well as time-dependent detector effects.

We use the Peterson fragmentation function [15] as a function of $x_E = 2E_{\mathrm{hadron}}/\sqrt{s}$ with the parameters $\epsilon_{\mathrm{b}} = 0.05$ and $\epsilon_{\mathrm{c}} = 0.50$ to describe the fragmentation of b and c quarks. We also use the L3 measurement, averaged with those from PEP and PETRA, of $\mathrm{Br}(\mathrm{b} \to \ell\nu\mathrm{X}) = 0.117 \pm 0.006$ [16] and take $\mathrm{Br}(\mathrm{c} \to \ell\nu\mathrm{X}) = 0.096 \pm 0.006$ from measurements at PETRA and PEP [17]. We use this value of $\mathrm{Br}(\mathrm{c} \to \ell\nu\mathrm{X})$ for both the prompt $\mathrm{c} \to \ell$ decay as well as for the cascade $\mathrm{b} \to \mathrm{c} \to \ell$ decay. To account for the uncertainty in the mixture of c-hadrons, and for the difference with low energy experiments, this branching is varied by 2 σ to compute the systematic error.

The lepton momentum spectra in JETSET from semileptonic decays of b and c hadrons do not completely agree with the data. We therefore reweight such events using the lepton momentum in the rest frame of the b or c hadron. We follow the procedure suggested by the LEP Electroweak Working Group on Heavy Flavours [18]. The lepton spectrum has to be corrected for 3 categories of events, $\mathrm{b} \to \ell$, $\mathrm{c} \to \ell$ and $\mathrm{b} \to \mathrm{c} \to \ell$.

For the $\mathrm{b} \to \ell$ spectrum we use 3 different models as suggested by the CLEO Collaboration [19]:

- The ACCMM model [20] with two parameters: the Fermi momentum $p_f = 298$ MeV and the mass of the produced quark $m_c = 1673$ MeV.

- The ISGW model [21] with the original model prediction of 11% D^{**} production.

- A modified version of the ISGW model (ISGW**) with 32% D^{**} production as measured by the CLEO Collaboration [19] .

For completeness, we show the results for all three models, although we take the ACCMM model for our central values, and use the ISGW and ISGW** models to estimate the systematic error due to the b decay models.

For the $\mathrm{c} \to \ell$ spectrum we use the data from DELCO [22] and MARK III [23], which we fit to the spectrum of the ACCMM model, including the effects of detector resolution and radiative corrections. The main uncertainty in this spectrum comes from the experimental measurements. We have investigated the best way to parameterize the dependence of the measured asymmetry and mixing on this uncertainty and found that varying p_f by $\pm 1\sigma$ is a good estimate [18].

For the $\mathrm{b} \to \mathrm{c} \to \ell$ decays we correct the c hadron momentum spectrum using the measured CLEO spectra for inclusive D^0 and D^+ coming from B decays [24] and correct the lepton momentum spectrum from the c hadron decays using the procedure above. The uncertainty introduced in the lepton spectrum due to the c hadron spectrum is small. $\mathrm{D_s}$ mesons are produced from $\mathrm{B_s}$ as well as from $\mathrm{B_u}$ and $\mathrm{B_d^0}$ mesons. In order to take into account possible differences in the $\mathrm{D_s}$ momentum spectra from these different mesons, we have investigated the effect on the result of not reweighting the spectrum and reweighting it according to the CLEO D^0 and D^+ spectrum from B mesons. Leptons from baryons are assumed to have the same spectra as those from the corresponding mesons, which should be the case if the leptons come from W decay via the spectator mechanism.

Monte Carlo events with single leptons are classified into six categories: $b \to \ell$, $b \to c \to \ell$, $b \to \tau \to \ell$, $b \to c\bar{c}s$ where $\bar{c} \to \ell$, $c \to \ell$, and background. Included in the background are leptons from π and K decays, Dalitz decays, photon conversions and misidentified hadrons caused by, for example, $\pi - \gamma$ overlap for electrons and punchthrough for muons.

We determine that the efficiency for observing a prompt $b \to \ell$ decay is 34% for muons and 20% for electrons. The efficiency varies by about 1% for the muons and 0.5% for electrons depending on the decay model used. The sample purities are shown in Table 2 for single lepton events and in Table 3 for dilepton events.

Category	μ	e
$b \to \ell$	65.2%	79.3%
$b \to c \to \ell$	7.8%	5.4%
$b \to \tau \to \ell$	1.9%	1.9%
$b \to \bar{c} \to \ell$	0.7%	0.3%
$c \to \ell$	9.2%	4.0%
background	15.2%	9.1%

Table 2: Monte Carlo estimates of the fraction of each process in the single lepton data sample.

Category	$\mu\mu$	ee	μe
$b \to \ell$, $b \to \ell$	70.2%	81.2%	77.0%
$b \to c \to \ell$, $b \to c \to \ell$	1.0%	0.2%	0.6%
$b \to \ell$, $b \to c \to \ell$	16.3%	8.2%	14.1%
$b \to \ell$, $b \to$ background	5.2%	5.1%	3.6%
$b \to c \to \ell$, $b \to$ background	1.2%	1.3%	0.3%
$b \to$ background, $b \to$ background	0.1%	0.0%	0.0%
$c \to \ell$, $c \to \ell$	2.1%	0.0%	1.1%
background, background	3.9%	4.0%	3.3%

Table 3: Monte Carlo estimates of the sample purities for dilepton events. The $b \to \ell$ fraction includes also $b \to \bar{c} \to \ell$ and $b \to \tau \to \ell$.

Fitting Method

An unbinned maximum likelihood fit is performed using the p and p_t of each lepton to determine χ_{B} and $A_{b\bar{b}}$. This fit is described in detail in References 4 and 11. For each event its probability to arise from each source is computed using the number of Monte Carlo events in a box in p and p_t space. For the mixing, this box is four dimensional, using the p and p_t of the two leptons, whereas for the asymmetry it is two dimensional. Shown in Figure 1 are the p and p_t distributions for the selected electrons and muons along with the predicted Monte Carlo fractions from the various sources.

Determination of the Mixing Parameter

The signature for B^0-$\bar{B}^0$ mixing is hadronic events with two prompt leptons with the same charge on opposite sides of the event. The angle between the two leptons is required to be larger than 60° to ensure that they are from different b-hadron decays. In the case where there are more than two leptons in an event, the two with the highest transverse momentum are considered. The number of dilepton events in the sample is given in Table 1.

Using the ACCMM model to describe the lepton spectra, the result of the fit is

$$\chi_{\mathrm{B}} = 0.123 \pm 0.012\ (\text{stat.}) \pm 0.008\ (\text{sys.}). \tag{4}$$

Figure 2 shows the rate of same charge dilepton events over all dileptons as a function of the p_t of the least energetic lepton. Since the leptons are in opposite hemisphere, the plot shows the increase of the mixing effect when the p_t increases, *i.e.* when the sample is enriched in prompt $\mathrm{b} \to \ell$ events.

The values for the mixing parameter using the ISGW and ISGW** models are $\chi_{\mathrm{B}} = 0.124 \pm 0.012$ (stat.) and $\chi_{\mathrm{B}} = 0.123 \pm 0.012$ (stat.) respectively. A consistent result of 0.122 ± 0.012 (stat.) is obtained by using the factorized fit method described in Reference 12, where the p and p_t spectra for each lepton are assumed to be independent.

Table 4 lists the contributions to the systematic error in the χ_{B} measurement. The first category is the uncertainty on the measurement of the partial decay widths, semileptonic branching ratios, fragmentation parameters and asymmetry. The most important contribution comes from the uncertainty in the $\mathrm{c} \to \ell$ branching ratio, which represents the largest background to the prompt lepton signal. The second category is the uncertainty on the modelling of the decays as explained above. The $\mathrm{b} \to \ell$ decay model systematic error is the largest difference between the mixing parameter measured using the ACCMM model and the two other models (ISGW in this case). Misidentified leptons that come from b-quark decays have a correlation with the parent quark charge. This charge correlation of the b-quark background is determined from the Monte Carlo to be 65%.

Determination of the Forward-Backward Asymmetry

In the semileptonic decay of a b quark the charge of the detected lepton is directly correlated with the charge of the quark. We use the thrust axis to estimate the direction of the original quark. The thrust axis is oriented towards the hemisphere containing the negatively charged lepton (or opposite the positively charged lepton). With this convention, the thrust axis points in the direction of the b quark.

The result of the fit for $A_{\mathrm{b\bar{b}}}$ using both inclusive muons and electrons is

$$A_{\mathrm{b\bar{b}}}^{\mathrm{obs}} = 0.066 \pm 0.008, \tag{5}$$

where the error is statistical only. For this result, the lepton spectra are described using the ACCMM model. The values using the ISGW and ISGW** models are 0.066 ± 0.008 (stat.) and 0.066 ± 0.008 (stat.) respectively. Separate fits for $A_{\mathrm{b\bar{b}}}$ using the muon and electron data yield $A_{\mathrm{b\bar{b}}}^{\mathrm{obs}} = 0.072 \pm 0.010$ for muons, and 0.057 ± 0.012 for electrons. Figure 3 shows the angular distribution of the oriented thrust axis for electrons and muons. A fit to the combined distribution for electrons and muons gives a result of 0.064 ± 0.009, in good agreement with the unbinned maximum likelihood fit.

Contribution	Variation	$\Delta\chi_{\rm B}$ $\times 10^2$	$\Delta A_{\rm b\bar{b}}^{\rm obs}$ $\times 10^2$	$\Delta A_{\rm b\bar{b}}$ $\times 10^2$
$\Gamma_{\rm b\bar{b}}/\Gamma_{\rm had} = 0.216$	± 0.005	± 0.002	∓ 0.029	± 0.038
$\Gamma_{\rm c\bar{c}}/\Gamma_{\rm had} = 0.169$	± 0.005	± 0.002	± 0.020	± 0.027
$\mathrm{Br}(\mathrm{b} \to \ell\nu\mathrm{X}) = 0.117$	± 0.006	± 0.264	∓ 0.081	± 0.046
$\mathrm{Br}(\mathrm{c} \to \ell\nu\mathrm{X}) = 0.096$	± 0.012	∓ 0.511	± 0.155	± 0.088
$\epsilon_{\rm b} = 0.050$	± 0.010	± 0.075	∓ 0.028	± 0.019
$\epsilon_{\rm c} = 0.50$	± 0.20	∓ 0.006	± 0.019	± 0.024
$A_{\rm c\bar{c}} = 0.06$	± 0.015		± 0.104	± 0.138
Number of c quarks per b quark decay = 1.15	± 0.10	± 0.086	∓ 0.030	± 0.020
Monte Carlo Decay models				
b decay models		± 0.030	± 0.070	± 0.100
c decay model ($p_f = 0.467$ GeV)	± 0.114	± 0.186	∓ 0.070	± 0.049
B $\to$D X spectrum		± 0.127	∓ 0.022	± 0.000
B$\to$D$_{\rm s}$ weighting		± 0.085	± 0.018	± 0.043
Charge correlation of the b quark background: 0.65	± 0.15	∓ 0.178	± 0.019	± 0.016
Background fraction	$\pm 10\%$	∓ 0.059	± 0.039	± 0.038
$A_{\rm back} = 0.00$	± 0.015		∓ 0.150	± 0.199
Detector related uncertainties				
Charge confusion correction	± 0.0015	± 0.150	∓ 0.020	± 0.008
Smearing of the lepton momentum	$\pm 15\%$	± 0.300	± 0.030	± 0.108
Smearing of the angle between the lepton and the jet	1°	± 0.142	± 0.100	± 0.165
Monte Carlo statistics		± 0.313	± 0.150	± 0.212
Combined		± 0.82	± 0.34	± 0.42

Table 4: Systematic errors on the $\chi_{\rm B}$, $A_{\rm b\bar{b}}^{\rm obs}$ and $A_{\rm b\bar{b}}$ measurements.

Table 4 lists the contributions to the systematic error in the $A_{b\bar{b}}^{obs}$ measurement. The error due to the b-decay models is the difference between the central value and the value computed using the ISGW** model.

Correcting $A_{b\bar{b}}^{obs}$ using our measured value of χ_B given above, we obtain

$$A_{b\bar{b}} = 0.087 \pm 0.011\ (\text{stat.}) \pm 0.004\ (\text{sys.}).$$

In determining the systematic error for $A_{b\bar{b}}$, we have taken advantage of the fact that for many of the sources of systematic error, there is a partial cancellation in the ratio $A_{b\bar{b}}^{obs}/(1-2\chi_B)$. For example, a higher $b \to c \to \ell$ branching ratio would decrease $A_{b\bar{b}}^{obs}$, but increase χ_B. The last column in Table 4 gives the systematic error on $A_{b\bar{b}}$ taking this effect into account.

Determination of $\sin^2\overline{\theta}_W$

The Born level approximation for the asymmetry given in the introduction is only valid at the Z mass. In addition, one must apply QED initial and final state radiative corrections, as well as QCD corrections due to gluon bremsstrahlung.

The calculations of Djouadi *et al.* [25] are used to determine the QCD correction which amounts to a 3.1% relative change. We use the ZFITTER program [26] to calculate the QED corrections and the shift due to the difference between the center-of-mass energy and the Z mass, which is an absolute change in $A_{b\bar{b}}$ of +0.0021. The resulting Born level asymmetry is

$$A_{b\bar{b}}^0 = 0.092 \pm 0.012.$$

Within the Standard Model, the effective electroweak mixing angle can be extracted from $A_{b\bar{b}}^0$ and corresponds to

$$\sin^2\overline{\theta}_W = 0.2335 \pm 0.0021,$$

which is in excellent agreement with our measurement [27] of $\sin^2\overline{\theta}_W = 0.2312 \pm 0.0022$ from the leptonic and hadronic decays of the Z.

Conclusions

We have analyzed $Z \to b\bar{b}$ decays using inclusive lepton events selected from a sample of 1,044,000 hadronic events. From a fit to the p and p_t distributions for single lepton and dilepton events, we have determined the average B^0-$\bar{B}^0$ mixing parameter that corresponds to the composition of B_s^0 and B_d^0 states produced in Z decays to be

$$\chi_B = 0.123 \pm 0.012\ (\text{stat.}) \pm 0.008\ (\text{sys.}).$$

Combining this measurement with the B_d^0 mixing value measured by the CLEO Collaboration [28] $\chi_d = 0.157^{+0.037}_{-0.032}$, and assuming the fractions of B_d^0 and B_s^0 at LEP to be $f_d = 0.375 \pm 0.05$ and $f_s = 0.15 \pm 0.05$ [2], we extract a value for the B_s^0 mixing parameter of $\chi_s = 0.43^{+0.26}_{-0.17}$, compatible with the large mixing required for the unitarity of the CKM matrix.

The $b\bar{b}$ forward-backward asymmetry at the effective center-of-mass energy $\sqrt{s} = 91.30$ GeV is measured to be:

$$A_{b\bar{b}} = 0.087 \pm 0.011\ (\text{stat.}) \pm 0.004\ (\text{sys.}).$$

Using this value of $A_{b\bar{b}}$, we have determined $\sin^2\overline{\theta}_W$ to be

$$\sin^2\overline{\theta}_W = 0.2335 \pm 0.0021.$$

Acknowledgments

We wish to express our gratitude to the CERN accelerator divisions for the excellent performance of the LEP machine. We acknowledge the contributions of all the engineers and technicians who have participated in the construction and maintenance of this experiment. Those of us who are not from member states thank CERN for its hospitality and help.

The L3 Collaboration:

M.Acciarri,[26] A.Adam,[43] O.Adriani,[16] M.Aguilar-Benitez,[25] S.Ahlen,[10] J.Alcaraz,[17] A.Aloisio,[28] G.Alverson,[11] M.G.Alviggi,[28] G.Ambrosi,[33] Q.An,[18] H.Anderhub,[46] A.L.Anderson,[15] V.P.Andreev,[37] T.Angelescu,[12] L.Antonov,[40] D.Antreasyan,[8] G.Alkhazov,[37] P.Arce,[25] A.Arefiev,[27] T.Azemoon,[3] T.Aziz,[9] P.V.K.S.Baba,[18] P.Bagnaia,[36] J.A.Bakken,[35] L.Baksay,[42] R.C.Ball,[3] S.Banerjee,[9] K.Banicz,[43] R.Barillère,[17] L.Barone,[36] A.Baschirotto,[26] M.Basile,[8] R.Battiston,[33] A.Bay,[19] F.Becattini,[16] U.Becker,[15] F.Behner,[46] Gy.L.Bencze,[13] J.Berdugo,[25] P.Berges,[15] B.Bertucci,[33] B.L.Betev,[40,46] M.Biasini,[33] A.Biland,[46] G.M.Bilei[33] R.Bizzarri,[36] J.J.Blaising,[4] G.J.Bobbink,[17,2] R.Bock,[1] A.Böhm,[1] B.Borgia,[36] D.Bourilkov,[46] M.Bourquin,[19] D.Boutigny,[17] B.Bouwens,[2] E.Brambilla,[15] J.G.Branson,[38] V.Brigljevic,[46] I.C.Brock,[34] M.Brooks,[23] A.Bujak,[43] J.D.Burger,[15] W.J.Burger,[19] C.Burgos,[25] J.Busenitz,[42] A.Buytenhuijs,[30] A.Bykov,[37] X.D.Cai,[18] M.Capell,[15] G.Cara Romeo,[8] M.Caria,[33] G.Carlino,[28] A.M.Cartacci,[16] J.Casaus,[25] R.Castello,[26] N.Cavallo,[28] M.Cerrada,[25] F.Cesaroni,[36] M.Chamizo,[25] Y.H.Chang,[48] U.K.Chaturvedi,[18] M.Chemarin,[24] A.Chen,[48] C.Chen,[6] G.Chen,[6,46] G.M.Chen,[6] H.F.Chen,[20] H.S.Chen,[6] M.Chen,[15] G.Chiefari,[28] C.Y.Chien,[5] M.T.Choi,[41] S.Chung,[15] L.Cifarelli,[8] F.Cindolo,[8] C.Civinini,[16] I.Clare,[15] R.Clare,[15] T.E.Coan,[23] H.O.Cohn,[31] G.Coignet,[4] N.Colino,[17] S.Costantini,[36] F.Cotorobai,[12] B.de la Cruz,[25] X.T.Cui,[18] X.Y.Cui,[18] T.S.Dai,[15] R.D'Alessandro,[16] R.de Asmundis,[28] A.Degré,[4] K.Deiters,[44] E.Dénes,[13] P.Denes,[35] F.DeNotaristefani,[36] D.DiBitonto,[42] M.Diemoz,[36] H.R.Dimitrov,[40] C.Dionisi,[36] M.Dittmar,[46] L.Djambazov,[46] M.T.Dova,[18,♯] E.Drago,[28] D.Duchesneau,[19] P.Duinker,[2] I.Duran,[39] S.Easo,[33] H.El Mamouni,[24] A.Engler,[34] F.J.Eppling,[15] F.C.Erné,[2] P.Extermann,[19] R.Fabbretti,[44] M.Fabre,[44] S.Falciano,[36] A.Favara,[16] J.Fay,[24] M.Felcini,[46] T.Ferguson,[34] D.Fernandez,[25] G.Fernandez,[25] F.Ferroni,[36] H.Fesefeldt,[1] E.Fiandrini,[33] J.H.Field,[19] F.Filthaut,[30] P.H.Fisher,[5] G.Forconi,[15] L.Fredj,[19] K.Freudenreich,[46] M.Gailloud,[22] Yu.Galaktionov,[27,15] E.Gallo,[16] S.N.Ganguli,[9] P.Garcia-Abia,[25] S.Gentile,[36] J.Gerald,[5] N.Gheordanescu,[12] S.Giagu,[36] S.Goldfarb,[22] Z.F.Gong,[20] E.Gonzalez,[25] A.Gougas,[5] D.Goujon,[19] G.Gratta,[32] M.W.Gruenewald,[17] C.Gu,[18] M.Guanziroli,[18] V.K.Gupta,[35] A.Gurtu,[9] H.R.Gustafson,[3] L.J.Gutay,[43] A.Hasan,[18] D.Hauschildt,[2] J.T.He,[6] T.Hebbeker,[7] M.Hebert,[38] A.Hervé,[17] K.Hilgers,[1] H.Hofer,[46] H.Hoorani,[19] S.R.Hou,[48] G.Hu,[18] B.Ille,[24] M.M.Ilyas,[18] V.Innocente,[17] H.Janssen,[4] B.N.Jin,[6] L.W.Jones,[3] P.de Jong,[15] I.Josa-Mutuberria,[17] A.Kasser,[22] R.A.Khan,[18] Yu.Kamyshkov,[31] P.Kapinos,[45] J.S.Kapustinsky,[23] Y.Karyotakis,[17] M.Kaur,[18] S.Khokhar,[18] M.N.Kienzle-Focacci,[19] D.Kim,[5] J.K.Kim,[41] S.C.Kim,[41] Y.G.Kim,[41] W.W.Kinnison,[23] A.Kirkby,[32] D.Kirkby,[32] S.Kirsch,[45] W.Kittel,[30] A.Klimentov,[15,27] A.C.König,[30] E.Koffeman,[2] O.Kornadt,[1] V.Koutsenko,[15,27] A.Koulbardis,[37] R.W.Kraemer,[34] T.Kramer,[15] V.R.Krastev,[40,33] W.Krenz,[1] H.Kuijten,[30] K.S.Kumar,[14] A.Kunin,[15,27] P.Ladron de Guevara,[25] G.Landi,[16] D.Lanske,[1] S.Lanzano,[28] A.Lebedev,[15] P.Lebrun,[24] P.Lecomte,[46] P.Lecoq,[17] P.Le Coultre,[46] D.M.Lee,[23] J.S.Lee,[41] K.Y.Lee,[41] I.Leedom,[11] C.Leggett,[3] J.M.Le Goff,[17] R.Leiste,[45] M.Lenti,[16] E.Leonardi,[36] P.Levtchenko,[37] C.Li,[20,18] W.T.Lin,[48] F.L.Linde,[2] B.Lindemann,[1] L.Lista,[28] Y.Liu,[18] W.Lohmann,[45] E.Longo,[36] W.Lu,[32] Y.S.Lu,[6] J.M.Lubbers,[17] K.Lübelsmeyer,[1] C.Luci,[36] D.Luckey,[15] L.Ludovici,[36] L.Luminari,[36] W.Lustermann,[44] W.G.Ma,[20] M.MacDermott,[46] L.Malgeri,[36] R.Malik,[18] A.Malinin,[27] C.Maña,[25] M.Maolinbay,[46] P.Marchesini,[46] F.Marion,[4] A.Marin,[10] J.P.Martin,[24] F.Marzano,[36] G.G.G.Massaro,[2] K.Mazumdar,[9] P.McBride,[14] T.McMahon,[43] D.McNally,[38] M.Merk,[34] L.Merola,[28] M.Meschini,[16] W.J.Metzger,[30] Y.Mi,[22] A.Mihul,[12] G.B.Mills,[23] Y.Mir,[18] G.Mirabelli,[36] J.Mnich,[1] M.Möller,[1] V.Monaco,[36] B.Monteleoni,[16] R.Morand,[4] S.Morganti,[36] N.E.Moulai,[18] R.Mount,[32] S.Müller,[1] E.Nagy,[13] M.Napolitano,[28] F.Nessi-Tedaldi,[46] H.Newman,[32] M.A.Niaz,[18] A.Nippe,[1] H.Nowak,[45] G.Organtini,[36] D.Pandoulas,[1] S.Paoletti,[36] P.Paolucci,[28] G.Pascale,[36] G.Passaleva,[16,33] S.Patricelli,[28] T.Paul,[5] M.Pauluzzi,[33] C.Paus,[1] F.Pauss,[46] Y.J.Pei,[1] S.Pensotti,[26] D.Perret-Gallix,[4] A.Pevsner,[5] D.Piccolo,[28] M.Pieri,[17] J.C.Pinto,[34] P.A.Piroué,[35] F.Plasil,[31] V.Plyaskin,[27] M.Pohl,[46] V.Pojidaev,[27,16] H.Postema,[15] N.Produit,[19] J.M.Qian,[3] K.N.Qureshi,[18] R.Raghavan,[9] G.Rahal-Callot,[46] P.G.Rancoita,[26] M.Rattaggi,[26] G.Raven,[2] P.Razis,[29] K.Read,[31] M.Redaelli,[26] D.Ren,[46] Z.Ren,[18] M.Rescigno,[36] S.Reucroft,[11] A.Ricker,[1] S.Riemann,[45] B.C.Riemers,[43] K.Riles,[3] O.Rind,[3] H.A.Rizvi,[18] S.Ro,[41] A.Robohm,[46] F.J.Rodriguez,[25] B.P.Roe,[3] M.Röhner,[1] S.Röhner,[1] L.Romero,[25] S.Rosier-Lees,[4] R.Rosmalen,[30] Ph.Rosselet,[22] W.van Rossum,[2] S.Roth,[1] A.Rubbia,[15] J.A.Rubio,[17] H.Rykaczewski,[46] M.Sachwitz,[45] J.Salicio,[17] J.M.Salicio,[25] E.Sanchez,[25] G.S.Sanders,[23] A.Santocchia,[33] M.E.Sarakinos,[43] G.Sartorelli,[18] M.Sassowsky,[1] G.Sauvage,[4] C.Schäfer,[1] V.Schegelsky,[37] D.Schmitz,[1] P.Schmitz,[1] M.Schneegans,[4] N.Scholz,[46] H.Schopper,[47] D.J.Schotanus,[30] S.Shotkin,[15] H.J.Schreiber,[45] J.Shukla,[34] R.Schulte,[1] K.Schultze,[1] J.Schwenke,[1] G.Schwering,[1] C.Sciacca,[28] I.Scott,[14] R.Sehgal,[18] P.G.Seiler,[44] J.C.Sens,[17,2] L.Servoli,[33] I.Sheer,[38] S.Shevchenko,[32] X.R.Shi,[32] E.Shumilov,[27] V.Shoutko,[27] D.Son,[41] A.Sopczak,[17] V.Soulimov,[28] C.Spartiotis,[21] T.Spickermann,[1] P.Spillantini,[16] M.Steuer,[15] D.P.Stickland,[35] F.Sticozzi,[15] H.Stone,[35] K.Strauch,[14] K.Sudhakar,[9] G.Sultanov,[18] L.Z.Sun,[20,18] G.F.Susinno,[19] H.Suter,[46] J.D.Swain,[18] A.A.Syed,[30] X.W.Tang,[6] L.Taylor,[11] R.Timellini,[8] Samuel C.C.Ting,[15] S.M.Ting,[15] O.Toker,[33] M.Tonutti,[1] S.C.Tonwar,[9] J.Tóth,[13] G.Trowitzsch,[45] A.Tsaregorodtsev,[37] G.Tsipolitis,[34] C.Tully,[35] T.Tuuva,[21] J.Ulbricht,[46] L.Urbán,[13] U.Uwer,[1] E.Valente,[36] R.T.Van de Walle,[30] I.Vetlitsky,[27] G.Viertel,[46] P.Vikas,[18] U.Vikas,[18] M.Vivargent,[4] H.Vogel,[34] H.Vogt,[45] I.Vorobiev,[14,27] A.A.Vorobyov,[37] An.A.Vorobyov,[37] L.Vuilleumier,[22] M.Wadhwa,[4] W.Wallraff,[1] J.C.Wang,[15] X.L.Wang,[20] Y.F.Wang,[15] Z.M.Wang,[18,20] A.Weber,[1] J.Weber,[46] R.Weill,[22] C.Willmott,[25] F.Wittgenstein,[17] D.Wright,[35] S.X.Wu,[18] S.Wynhoff,[1] Z.Z.Xu,[20] B.Z.Yang,[20] C.G.Yang,[6] G.Yang,[18] X.Y.Yao,[6] C.H.Ye,[18] J.B.Ye,[20] Q.Ye,[18] S.C.Yeh,[48] J.M.You,[18] N.Yunus,[18] M.Yzerman,[2] C.Zaccardelli,[32] P.Zemp,[46] M.Zeng,[18] Y.Zeng,[1] D.H.Zhang,[2] Z.P.Zhang,[20,18] B.Zhou,[10] G.J.Zhou,[6] J.F.Zhou,[1] R.Y.Zhu,[32] A.Zichichi,[8,17,18] B.C.C.van der Zwaan.[2]

1 I. Physikalisches Institut, RWTH, D-52056 Aachen, FRG§
III. Physikalisches Institut, RWTH, D-52056 Aachen, FRG§
2 National Institute for High Energy Physics, NIKHEF, NL-1009 DB Amsterdam, The Netherlands
3 University of Michigan, Ann Arbor, MI 48109, USA
4 Laboratoire d'Annecy-le-Vieux de Physique des Particules, LAPP,IN2P3-CNRS, BP 110, F-74941 Annecy-le-Vieux CEDEX, France
5 Johns Hopkins University, Baltimore, MD 21218, USA
6 Institute of High Energy Physics, IHEP, 100039 Beijing, China
7 Humboldt University, D-10099 Berlin, FRG
8 INFN-Sezione di Bologna, I-40126 Bologna, Italy
9 Tata Institute of Fundamental Research, Bombay 400 005, India
10 Boston University, Boston, MA 02215, USA
11 Northeastern University, Boston, MA 02115, USA
12 Institute of Atomic Physics and University of Bucharest, R-76900 Bucharest, Romania
13 Central Research Institute for Physics of the Hungarian Academy of Sciences, H-1525 Budapest 114, Hungary‡
14 Harvard University, Cambridge, MA 02139, USA
15 Massachusetts Institute of Technology, Cambridge, MA 02139, USA
16 INFN Sezione di Firenze and University of Florence, I-50125 Florence, Italy
17 European Laboratory for Particle Physics, CERN, CH-1211 Geneva 23, Switzerland
18 World Laboratory, FBLJA Project, CH-1211 Geneva 23, Switzerland
19 University of Geneva, CH-1211 Geneva 4, Switzerland
20 Chinese University of Science and Technology, USTC, Hefei, Anhui 230 029, China
21 SEFT, Research Institute for High Energy Physics, P.O. Box 9, SF-00014 Helsinki, Finland
22 University of Lausanne, CH-1015 Lausanne, Switzerland
23 Los Alamos National Laboratory, Los Alamos, NM 87544, USA
24 Institut de Physique Nucléaire de Lyon, IN2P3-CNRS,Université Claude Bernard, F-69622 Villeurbanne Cedex, France
25 Centro de Investigaciones Energeticas, Medioambientales y Tecnologicas, CIEMAT, E-28040 Madrid, Spain
26 INFN-Sezione di Milano, I-20133 Milan, Italy
27 Institute of Theoretical and Experimental Physics, ITEP, Moscow, Russia
28 INFN-Sezione di Napoli and University of Naples, I-80125 Naples, Italy
29 Department of Natural Sciences, University of Cyprus, Nicosia, Cyprus
30 University of Nymegen and NIKHEF, NL-6525 ED Nymegen, The Netherlands
31 Oak Ridge National Laboratory, Oak Ridge, TN 37831, USA
32 California Institute of Technology, Pasadena, CA 91125, USA
33 INFN-Sezione di Perugia and Universitá Degli Studi di Perugia, I-06100 Perugia, Italy
34 Carnegie Mellon University, Pittsburgh, PA 15213, USA
35 Princeton University, Princeton, NJ 08544, USA
36 INFN-Sezione di Roma and University of Rome, "La Sapienza", I-00185 Rome, Italy
37 Nuclear Physics Institute, St. Petersburg, Russia
38 University of California, San Diego, CA 92093, USA
39 Dept. de Fisica de Particulas Elementales, Univ. de Santiago, E-15706 Santiago de Compostela, Spain
40 Bulgarian Academy of Sciences, Institute of Mechatronics, BU-1113 Sofia, Bulgaria
41 Center for High Energy Physics, Korea Advanced Inst. of Sciences and Technology, 305-701 Taejon, Republic of Korea
42 University of Alabama, Tuscaloosa, AL 35486, USA
43 Purdue University, West Lafayette, IN 47907, USA
44 Paul Scherrer Institut, PSI, CH-5232 Villigen, Switzerland
45 DESY-Institut für Hochenergiephysik, D-15738 Zeuthen, FRG
46 Eidgenössische Technische Hochschule, ETH Zürich, CH-8093 Zürich, Switzerland
47 University of Hamburg, 22761 Hamburg, FRG
48 High Energy Physics Group, Taiwan, China
§ Supported by the German Bundesministerium für Forschung und Technologie
‡ Supported by the Hungarian OTKA fund under contract number 2970.
♯ Also supported by CONICET and Universidad Nacional de La Plata, CC 67, 1900 La Plata, Argentina

References

[1] S.L. Glashow, Nucl. Phys. **22** (1961) 579;
S. Weinberg, Phys. Rev. Lett. **19** (1967) 1264;
A. Salam, "Elementary Particle Theory", Ed. N. Svartholm, Stockholm, "Almquist and Wiksell" (1968), 367.

[2] J. Kühn and P. Zerwas, "Heavy Flavors at LEP I" Preprint MPI-PAE/PTh 49/89, Max Planck Institute, Munich. A shortened version is available as J. Kühn and P. Zerwas in "Z Physics at LEP 1", CERN 89-08, ed. G. Altarelli *et al.*, (CERN, Geneva, 1989), volume 1, p. 267.

[3] M. Böhm and W. Hollik, in "Z Physics at LEP 1", CERN 89-08, ed. G. Altarelli, R. Kleiss and C. Verzegnassi, (CERN, Geneva, 1989), volume 1, p. 203.

[4] L3 Collab., B. Adeva *et al.*, Phys. Lett. **B 252** (1990) 713.

[5] MARK II Collab., J.F. Kral *et al.*, Phys. Rev. Lett. **64** (1990) 1211.

[6] OPAL Collab., R. Akers, *et al.*, Z. Phys. **C 60** (1993) 601;
OPAL Collab., R. Akers, *et al.*, Z. Phys. **C 60** (1993) 199;
OPAL Collab., P. D. Acton, *et al.*, Z. Phys. **C 60** (1993) 19;
OPAL Collab., P. D. Acton, *et al.*, Phys. Lett. **B 276** (1992) 379;
OPAL Collab., M. Z. Akrawy, *et al.*, Phys. Lett. **B 263** (1991) 311.

[7] ALEPH Collab., D. Buskulic, *et al.*, Preprint CERN-PPE/94-17, CERN, 1994;
ALEPH Collab., D. Buskulic, *et al.*, Phys. Lett. **B 284** (1992) 177;
ALEPH Collab., D. Decamp, *et al.*, Phys. Lett. **B 263** (1991) 325.

[8] DELPHI Collab., P. Abreu, *et al.*, Preprint CERN-PPE/94-67 , CERN, 1994;
DELPHI Collab., P. Abreu, *et al.*, Preprint CERN-PPE/93-220, CERN, 1994;
DELPHI Collab., P. Abreu, *et al.*, Phys. Lett. **B 301** (1993) 145;
DELPHI Collab., P. Abreu, *et al.*, Phys. Lett. **B 276** (1992) 536.

[9] O. Adriani *et al.*, Nucl. Inst. Meth. **A 302** (1991) 53.

[10] L3 Collab., B. Adeva *et al.*, Nucl. Inst. Meth. **A 289** (1990) 35.

[11] L3 Collab., B. Adeva *et al.*, Phys. Lett. **B 252** (1990) 703.

[12] L3 Collab., B. Adeva *et al.*, Phys. Lett. **B 288** (1992) 395.

[13] T. Sjöstrand, Comp. Phys. Comm. **39** (1986) 347;
T. Sjöstrand and M. Bengtsson, Comp. Phys. Comm. **43** (1987) 367.

[14] The L3 detector simulation is based on GEANT Version 3.15.
See R. Brun *et al.*, "GEANT 3", CERN DD/EE/84-1 (Revised), September 1987.
The GHEISHA program (H. Fesefeldt, RWTH Aachen Report PITHA 85/02 (1985)) is used to simulate hadronic interactions.

[15] C. Peterson *et al.*, Phys. Rev. **D 27** (1983) 105.

[16] L3 Collab., B. Adeva *et al.*, Phys. Lett. **B 261** (1991) 177.

[17] Particle Data Group, Phys. Rev. **D 45** (1992) III.54.

[18] The LEP Electroweak Working Group on Heavy Flavours, "A Consistent Treatment of Systematic Errors for LEP Electroweak Heavy Flavour Analyses", Preprint L3 Note 1577, CERN, 1994.

[19] CLEO Collab., S. Henderson *et al.*, Phys. Rev. **D 45** (1992) 45.

[20] G. Altarelli, N. Cabibbo, G. Carbó, L. Maiani and G. Martinelli, Nucl. Phys. **B 208** (1982) 365.

[21] N. Isgur *et al.*, Phys. Rev. **D 39** (1989) 799.

[22] W. Bacino *et al.*, Phys. Rev. Lett. **43** (1979) 1073.

[23] R.M. Baltrusaitis *et al.*, Phys. Rev. Lett. **54** (1985) 1976.

[24] CLEO Collab., D. Bortoletto *et al.*, Phys. Rev. **D 45** (1992) 21.

[25] A. Djouadi *et al.*, Z. Phys. **C 46** (1990) 411.

[26] D. Bardin *et al.*, FORTRAN package ZFITTER, and preprint CERN–TH. 6443/92;
D. Bardin *et al.*, Z. Phys. **C 44** (1989) 493;
D. Bardin *et al.*, Nucl. Phys. **B 351** (1991) 1;
D. Bardin *et al.*, Phys. Lett. **B 255** (1991) 290.

[27] L3 Collab., M. Acciarri *et al.*, "Measurement of Cross Sections and Leptonic Forward-Backward Asymmetries at the Z Pole and Determination of Electroweak Parameters", Preprint CERN-PPE/94-45, CERN, 1994, submitted to Z. Phy. C.

[28] CLEO Collab., J. Bartelt *et al.*, Phys. Rev. Lett. **71** (1993) 1680.

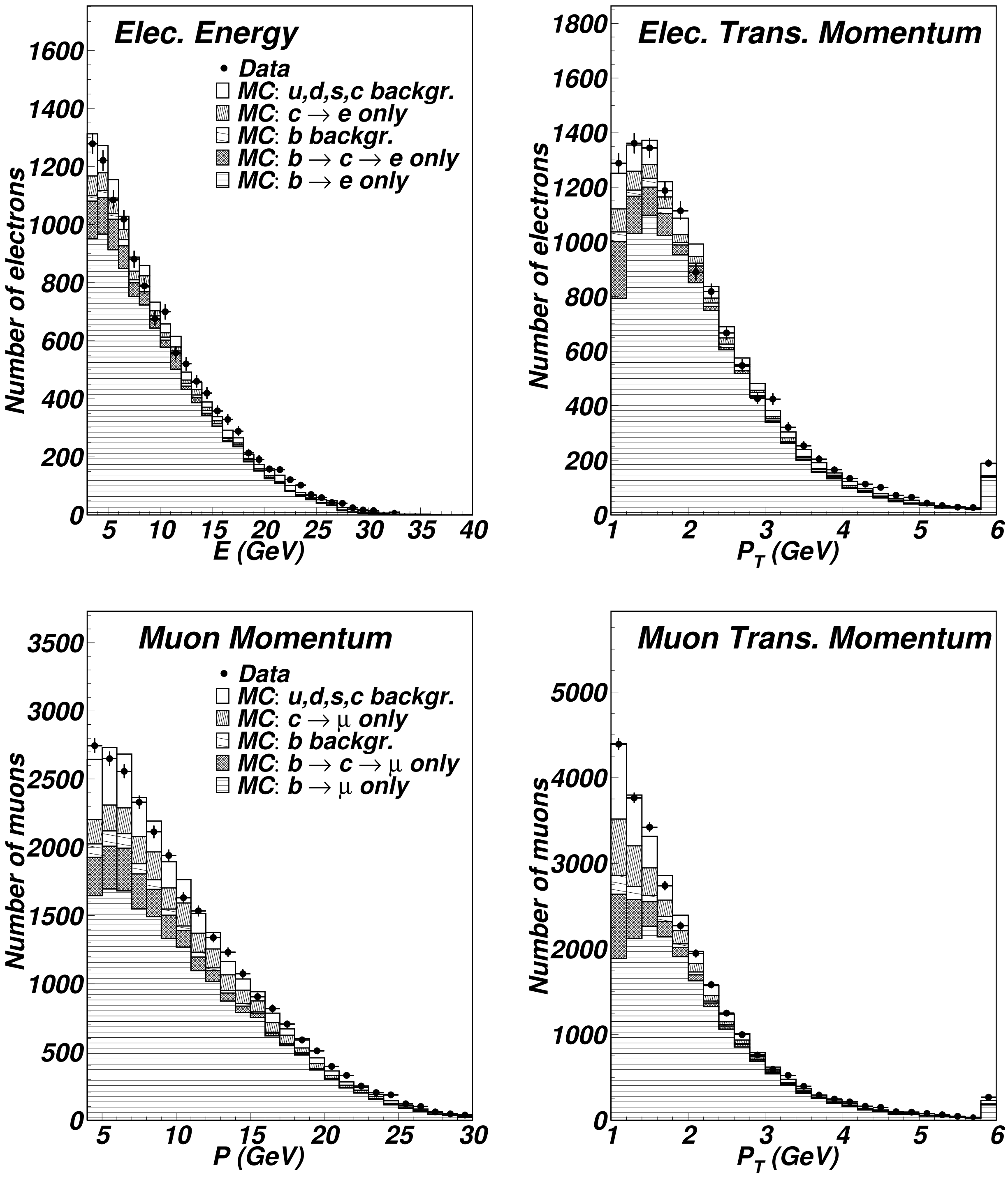

Figure 1: The p and p_t distributions for electrons and for muons. The contributions of the various sources are indicated. All leptons above 6 GeV p_t have been grouped into the last bin for the plot only.

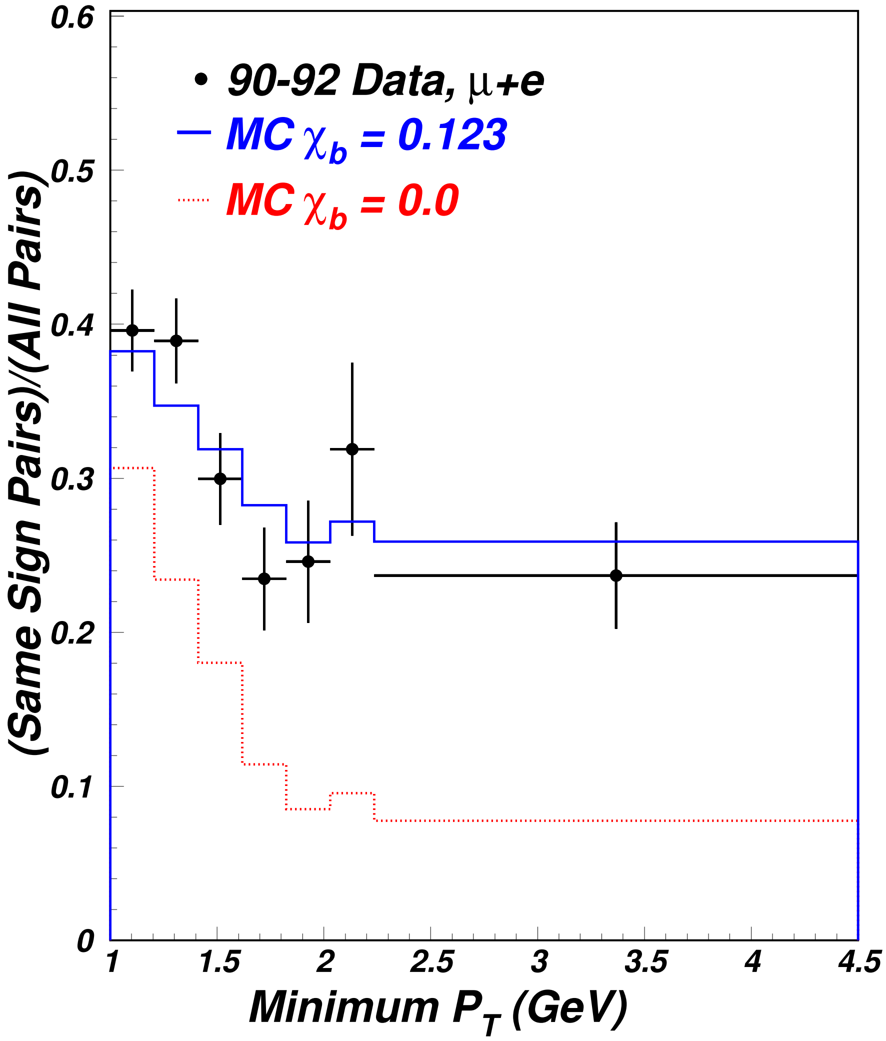

Figure 2: Ratio of same charge dileptons over all dileptons as a function of the transverse momentum of the less energetic lepton. The leptons are in opposite hemispheres. The curves are the Monte-Carlo expectations with no mixing (dotted line) and with the measured mixing (full line).

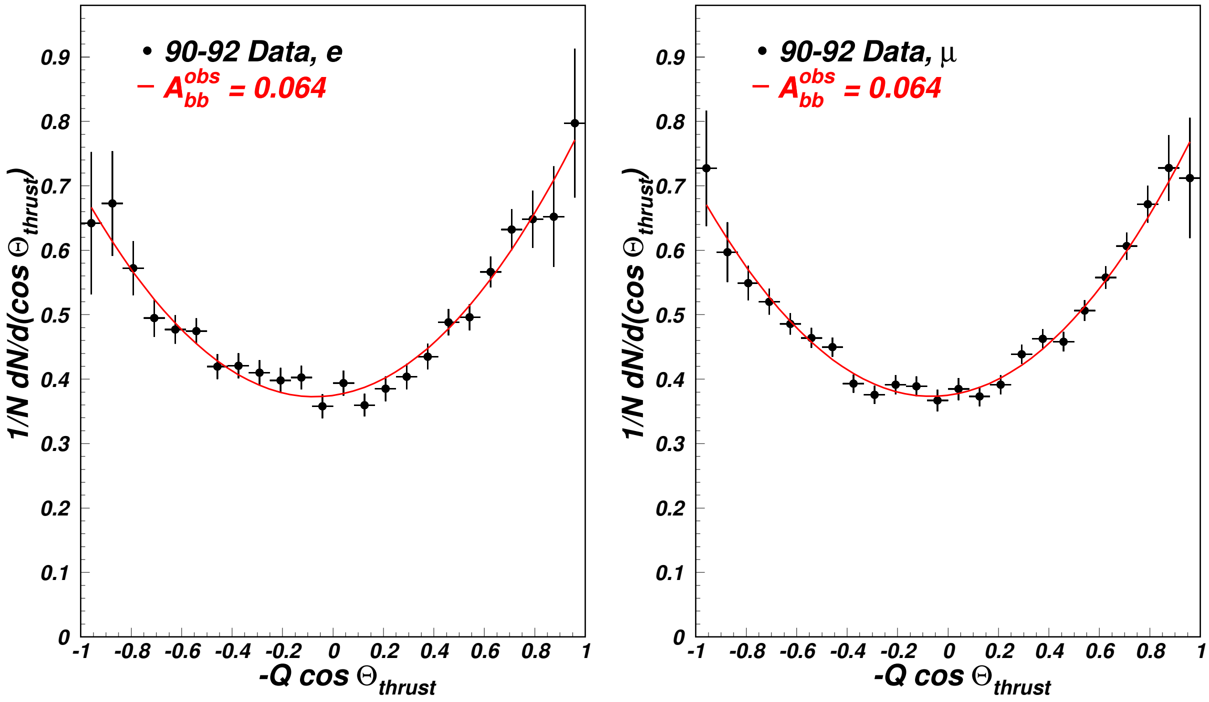

Figure 3: The measured angular distribution of the thrust axis for events containing a high p_t lepton (> 1 GeV) signed with the charge of the lepton for electrons and for muons. The distribution is corrected for acceptance and the background is subtracted. The measured asymmetry is from the fit to the combined electron and muon samples.